Inorganic Chemistry

Article

pubs.acs.org/IC

Solid-State Crystal-to-Crystal Phase Transitions and Reversible Structure–Temperature Behavior of Phosphovanadomolybdic Acid, $H_5PV_2Mo_{10}O_{40}$

Delina Barats-Damatov,[†] Linda J. W. Shimon,[‡] Yishay Feldman,[‡] Tatyana Bendikov,[‡] and Ronny Neumann*,[†]

[†]Department of Organic Chemistry, Weizmann Institute of Science, Rehovot 76100, Israel

[‡]Chemical Research Support Unit, Weizmann Institute of Science, Rehovot 76100, Israel

Supporting Information

ABSTRACT: The crystal packing and secondary structure of $H_5PV_2Mo_{12}O_{40}$ was followed by careful X-ray diffraction studies that revealed four unique structures and three solid phase transitions at temperatures between 25 and 55 °C, with loss of solvated water and concomitant contraction of the volume and increase of the packing density. Above 60 °C $H_5PV_2Mo_{12}O_{40}$ becomes amorphous and then anhydrous although the polyoxometalate cluster is stable indefinitely up to 300 °C. Above this temperature, combined IR, Raman, XRD, and XPS measurements show the decomposition of $H_5PV_2Mo_{12}O_{40}$ to crystalline MoO_3 and probably amorphous vanadium oxide and vanadylphosphate, the latter appearing to cover the surface of MoO_3. Importantly, $H_5PV_2Mo_{12}O_{40}$ can be easily recovered by dissolution in water at 80 °C.

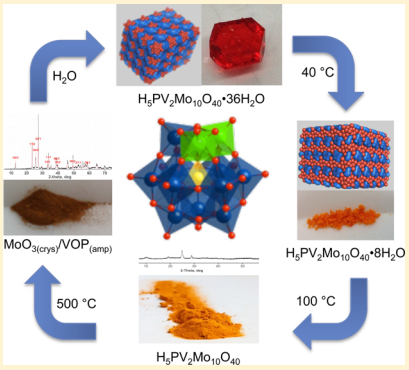

INTRODUCTION

Polyoxometalates are a versatile class of inorganic metal oxide compounds that have been extensively studied over last 80 years. In recent years, the general availability of high quality X-ray diffractometers has led to a plethora of new compounds and crystal structures. Polyoxometalates, typically synthesized by "self-assembly" of monomeric salts, often contain water molecules as an integral part of their structure. It is not uncommon for polyoxometalate based structures to have 10 or more structural water molecules[1] that together with counter cations form a so-called "secondary structure" in the solid state.[2] Since heterogeneous catalysis is one area where polyoxometalates have found widespread application,[3] the secondary structure may play a crucial role their activity and stability.

In the past, some studies on the thermal behavior of polyoxometalates have been performed[4] that included also various levels of characterization of structural water using numerous analytic techniques such as thermogravimetric analysis (TG),[5] differential thermal analysis (DTA),[6] X-ray diffraction measurements (XRD), Raman spectroscopy,[7] and infrared spectroscopy (IR).[8] Sometimes due to the lack of advanced crystallographic software and hardware and also crystal disorder, the secondary structure of crystals has been difficult to measure and solve. Thus, despite the importance of these structural water molecules, there are only few examples in the literature describing precise structural transformations within crystal lattices due to different degrees of hydration in polyoxometalate compounds. For instance, Günter and Bensch reported a single crystal structure of $Mg_8SiW_9O_{37}\cdot 24.5H_2O$, which was thermally and reversibly dehydrated to yield another crystal structure $Mg_8SiW_9O_{37}\cdot 12H_2O$.[9] Recently, Gutiérrez-Zorrilla and co-workers published two papers on reversible dehydration of Keggin-type hybrid organic–polyoxometalate compounds.[10] Significant structural changes in the packing arrangement emerged as a result of removal of a single water molecule.

We and others have been interested in the use phosphovanadomolybdates in heterogeneous and homogeneous catalysis, notably the very active $H_5PV_2Mo_{12}O_{40}$.[11] $H_5PV_2Mo_{12}O_{40}$ catalyzes many reactions that proceed through electron transfer and electron transfer–oxygen transfer (ET-OT) mechanisms.[12] Several reports on the thermal stability of such phosphorus containing polyoxometalates, mainly using powder X-ray analysis and thermogravimetric analysis, have appeared in order to determine the crystal lattice and degree of hydration.[13] For example, for $H_4PVMo_{11}O_{40}$, a 13-hydrate evolved from a 29-hydrate and a ~7–8-hydrate was proposed as an unstable species formed at 60–70 °C.[14] The dehydration process was also shown to be at least partially reversible.

Here, we present the first systematic study on divanado-substituted phosphomolybdic acid, $H_5PV_2Mo_{12}O_{40}$, with four different fully refined crystal structures, depending on the degree of hydration, from 36- to 8-hydrate. The process of dehydration proceeds via solid-state crystal-to-crystal trans-

Received: October 26, 2014
Published: January 7, 2015

DOI: 10.1021/ic502541b
Inorg. Chem. 2015, 54, 628–634

Table 1. Crystallographic Data for Compounds 1, 2, 3, 4, and 5

	1	2	3	4	5
formula	$Mo_{10}V_2PO_{76}H_{77}$	$Mo_{10}V_2PO_{76}H_{33}$	$Mo_{10}V_2PO_{76}H_{21}$	$Mo_{10}V_2PO_{76}H_{21}$	$Mo_{10}V_2PO_{76}H_{77}$
formula wt (g mol^{-1})	2349.58	1989.51	1881.42	1881.42	2349.58
cryst syst	monoclinic	triclinic	triclinic	triclinic	monoclinic
space group	$P2_1/n$	$P\bar{1}$	$P\bar{1}$	$P\bar{1}$	$P2_1/n$
T (K)	120(2)	120(2)	313(2)	120(2)	120(2)
a (Å)	12.7501(1)	13.4705(2)	9.7580(4)	13.4794(2)	12.748(3)
b (Å)	12.7512(1)	13.9620(2)	9.7627(6)	13.5005(3)	12.745(3)
c (Å)	18.0360(2)	13.9967(1)	9.8748(5)	13.9131(3)	18.027(4)
α (deg)	90.00	60.8204(8)	88.062(3)	61.6380(11)	90.00
β (deg)	90.010(6)	67.8345(8)	88.477(4)	61.0520(11)	90.06(3)
γ (deg)	90.00	70.3150(7)	89.832(4)	60.5232(12)	90.00
V (Å^3)	2932.28(5)	2090.11(5)	939.85(8)	1833.15(6)	2928.9(10)
Z	2	2	1	2	2
D_{calc} (g cm^{-3})	2.661	3.161	3.324	3.409	2.664
μ (mm^{-1})	2.544	3.501	3.871	3.969	2.547
collected reflns	65876	18248	7307	16017	59031
unique reflns	6729	9538	3832	8416	5848
R_{int}	0.0179	0.0406	0.0417	0.0434	0.0432
reflns [$I > 2\sigma(I)$]	5536	7025	2559	5967	4653
params	277	534	294	510	331
$R(F)^a$ [$I > 2\sigma(I)$]	0.0817	0.0689	0.0859	0.0558	0.0678
$wR(F^2)^a$ (all data)	0.2312	0.1817	0.2417	0.1420	0.1861
GOF	1.120	1.125	1.133	1.054	1.057

$^a R(F) = \sum||F_o| - |F_c||/\sum|F_o|$. $wR(F^2) = \{\sum[w(F_o^2 - F_c^2)^2]/\sum[w(F_o^2)^2]\}^{1/2}$.

formation and is fully reversible. The thermal stability of $H_5PV_2Mo_{12}O_{40}$ at high temperature, its degradation, and its complete recombination from simple oxides is also discussed.

EXPERIMENTAL SECTION

Materials and Methods. All chemicals were commercially purchased and used without further purification. $H_5PV_2Mo_{10}O_{40}$ was synthesized by a known literature procedure[15] and identified by ^{31}P NMR and infrared (FT-IR) spectroscopy. Crystals were grown and a large red crystal (1 cm × 1 cm), Figure S1, Supporting Information, was collected after 1 week in a desiccator from a concentrated aqueous solution and stored in its mother liquor. To prevent ambiguity, all crystal structures and subsequent research described in this work were carried out using this single "mother crystal". The original "wet" compound, $H_5PV_2Mo_{10}O_{40}\cdot 36H_2O$ (**1**), was measured as is. An air-dried compound, $H_5PV_2Mo_{10}O_{40}\cdot 14H_2O$ (**2**), was obtained by exposure of a piece of the mother crystal to an ambient atmosphere of 23 °C for 24 h. A further dehydrated compound, $H_5PV_2Mo_{10}O_{40}\cdot 8H_2O$, was prepared by heating a piece of the original crystal in an oven at 40 °C for overnight. Here two different structures were obtained (**3** and **4**), which were observed by X-ray diffraction measurements at 313 and 120 K, respectively. Heating a sample of the polyoxometalate at 100 °C for 18 h yielded an amorphous "dry" orange powder. Placement of this orange powder in a hydration vessel, Figure S2, Supporting Information, at room temperature for 2 h yielded small, rehydrated crystals (**5**) that were identical to (**1**). The number of water molecules in all the structures was confirmed by thermogravimetric analysis.

Characterization. Amorphous $H_5PV_2Mo_{10}O_{40}$. IR (cm^{-1}): 1060 (s), 961 (s), 864 (b), 778 (b), 594 (w). ^{31}P NMR (D2O, 400 MHz): δ −3.58 (s), δ −3.72 (s), δ −3.76 (s), δ −3.84 (s), δ −3.97 (s). Elemental analysis, calcd (exp): V 5.86 (5.81), Mo 55.23 (55.78). $H_5PV_2Mo_{10}O_{40}$ calcinated at 500 °C, **6**. IR (cm^{-1}): 1020 (w), 991 (s), 885 (b), 817 (w), 598 (b). ^{31}P NMR (D2O, 400 MHz): δ −3.58 (s), δ −3.72 (s), δ −3.76 (s), δ −3.84 (s), δ −3.97 (s). Elemental analysis, calcd for $PV_2Mo_{10}O_{37.5}$ (exp): V 6.02 (5.90), Mo 56.70 (57.11).

Instrumentation. ^{31}P and ^{51}V NMR spectra were recorded on Bruker Avance III 400 and Bruker Avance DPX 500 spectrometers using H_3PO_4 and $VOCl_3$, respectively, as external standards. IR spectra were measured on a Nicolet 6700 FT-IR spectrophotometer, deposited on NaCl plates. Elemental analyses were carried out on an Agilent 7700s ICP-MS. TG analyses were performed on a TA Instruments SDT Q600 thermobalance in flowing N_2, with a heating rate of 5 °C/min. Raman spectra were acquired from solid samples on a Renishaw Micro Raman Imaging microscope using a 633 nm laser. Powder X-ray diffraction (PXRD) patterns were collected on Rigaku ULTIMA III (2 kW) θ–θ vertical diffractometer equipped with sealed Cu-anode tube (λ = 0.154 nm) and Dectris X-ray strip detector Mythen1k (Switzerland). The measurements were carried out in a specular diffraction (2Θ/Θ scan) mode using nearly parallel X-ray beam focused by cross beam optics (CBO). Samples were placed in a temperature chamber filled with N_2; the temperature was controlled by a programmable temperature controller PTC-30. Phase analysis was made using the Jade 9.5 software (Materials Data) and PDF-4+ 2013 database (ICDD). XPS measurements were carried out with a Kratos AXIS ULTRA system using a monochromatic Al Kα X-ray source ($h\nu$ = 1486.6 eV) at 75 W and detection pass energies ranging between 20 and 80 eV. A low-energy electron flood gun (eFG) was applied for charge neutralization. To define binding energies (BE) of different elements, the C 1s line of contaminant carbon at 284.8 eV was taken as a reference.

X-ray Crystallography. Crystals were coated in Paratone-N oil (Hampton Research) and mounted within a MiTeGen cryo-loop. Single crystal X-ray data was collected on Nonius Kappa CCD diffractometer with Mo Kα (λ = 0.71073 nm) radiation. The data were processed using Denzo-scalepack.[16] Structures were solved by direct methods with SHELXS.[17] Full-matrix least-squares refinement was based on F^2 with SHELX-2013. The vanadium atomic positions were disordered over all 12 metal sites, so occupancy was constrained to a total of two atoms per molecule. Water molecules were placed automatically into the difference electron density map using cutoff criteria of 1.2σ as implemented in the water location routine of Coot.[18] Water occupied interstitial space between the polyanions within the crystal packing was calculated using HOLLOW[19] and visualized in PyMol.[20] The crystallographic data are presented in Table 1.

DOI: 10.1021/ic502541b
Inorg. Chem. 2015, 54, 628–634

RESULTS AND DISCUSSION

Crystal Structures. *$H_5PV_2Mo_{10}O_{40}\cdot 36H_2O$ (1).* Freshly prepared phosphovanadomolybdic acid yields intensely colored red crystals, Figure 1A, that crystallized in the monoclinic space

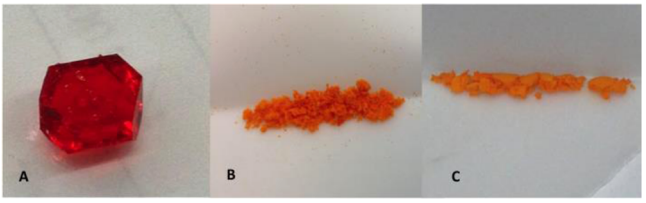

Figure 1. (A) $H_5PV_2Mo_{10}O_{40}\cdot 36H_2O$, (B) $H_5PV_2Mo_{10}O_{40}\cdot 14H_2O$, and (C) anhydrous $H_5PV_2Mo_{10}O_{40}$.

group $P2_1/n$ and contains two polyanions in the unit cell, Figure 2, left. This polyanion has the characteristic α-Keggin

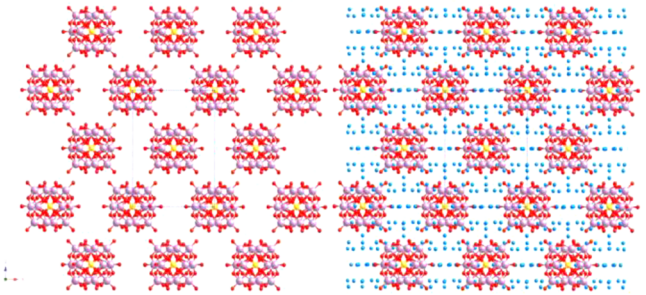

Figure 2. Crystal packing of **1** viewed along the *b* axis, without (left) and with (right) structural water molecules. Color code: M (Mo and V) pink, P yellow, and O red; water molecules are labeled blue for better presentation.

structure consisting of a central PO_4 tetrahedron surrounded by 12 MO_6 octahedra (M = Mo or V) arranged in four edge-shared M_3O_9 triads. The triads are linked together and with the PO_4 tetrahedron via corner sharing. In this crystal structure, the central PO_4 unit is disordered as indicated by the fact that P is surrounded by a cube of eight O atoms, each of them only half-occupied. This type of disorder is known for Keggin structures.[21]

There are five inseparable isomers in the $H_5PV_2Mo_{10}O_{40}$ core structure that are differentiated by the relative positions of the two vanadium atoms, Figure S3, Supporting Information. Thirty-six water molecules surround each Keggin cluster, and the average distance between the centers of the neighboring polyanions is 12.75 Å (averaged over six closest spheres), Figure 2, right. This structure was previously reported by Sergienko et al. in 1980,[22] crystallized in tetragonal space group *P4/mnc*, also having 36 water molecules. Here, although cell dimensions are nearly tetragonal, the structure refined better in a monoclinic space group.

$H_5PV_2Mo_{10}O_{40}\cdot 14H_2O$ (2). When exposed to air, **1** immediately starts to lose structural water molecules and breaks apart, and the red translucent crystal appears as an orange crystalline powder, Figure 1B. Every small crystallite in this powder diffracts well to yield the air-dried compound, **2**. The Keggin polyanion units in **2** are shifted toward one another and are arranged in a triclinic $P\bar{1}$ space group, as seen in Figure 3. The central PO_4 unit is not disordered in this case, and tetragonal coordination can be clearly observed. There are also

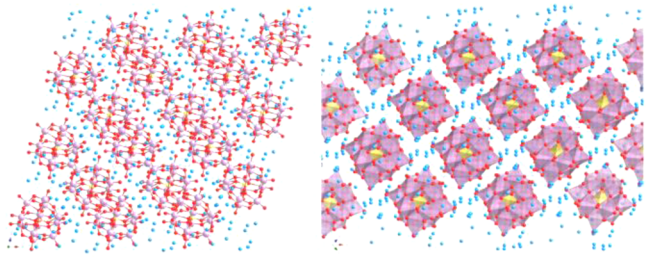

Figure 3. Crystal packing of **2** in ball and stick (left) and polyhedral (right) models, viewed along the *b* axis (left) and as projection of the {011} plane (right). Color code: M (Mo and V) pink, P yellow, and O red; water molecules are labeled blue for better representation.

two polyoxometalate clusters per unit cell; however, the distance between the neighboring polyanions was shortened to 10.29 Å, and the volume of the unit cell decreased by approximately 30% from 2932 to 2090 Å^3. There are 14 water molecules per each polyoxometalate unit in **2** that are positioned in a channel-like manner between the layers of Keggin polyanions.

$H_5PV_2Mo_{10}O_{40}\cdot 8H_2O$ (3). Compound **3** was obtained by drying the original crystal, **1**, at 40 °C. The crystal structure, also measured at this temperature, shows that there has been a unit cell transformation so that it is in a triclinic $P\bar{1}$ space group with one Keggin cluster per unit cell, Figure 4. Geometrically

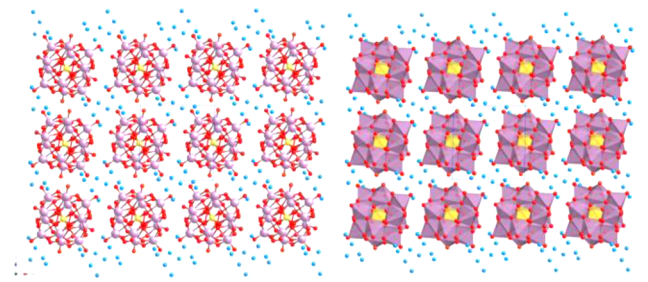

Figure 4. Crystal packing of **3** viewed along the *b* axis, in ball and stick (left) and polyhedral (right) models. Color code: M (Mo and V) pink, P yellow, and O red; structural water molecules are labeled blue for better representation.

this structure is nearly cubic. There remain only eight water molecules per cluster, and the volume of the unit cell contracted to 939.8 Å^3. The polyanions in **3** are packed very tightly in all three directions, leading to an average center-to-center distance between the neighboring polyoxometalates of 9.8 Å. The water molecules are located in small pockets, which are trapped between the Keggin polyanions and are aligned along the *c* axis. Interestingly, when the X-ray diffraction measurements were carried out at a lower temperature, 120 K, the compound undergoes a packing change and a new octahydrate structure (**4**) is formed.

$H_5PV_2Mo_{10}O_{40}\cdot 8H_2O$ (4). When the crystals of **1** were dried at 40−55 °C and then measured at 120 K, they formed a very tightly packed structure, **4**, Figure 5. Although crystallographically primitive with a triclinic, $P\bar{1}$ space group, geometrically this structure is nearly rhombohedral with α (61.6) ≈ β (61.1) ≈ γ (60.5) and a (13.5) ≈ b (13.5) ≈ c (13.9). The packing arrangement of **4** is dense and resembles a hexagonal closed packed structure of equal spheres. Assuming a spherical geometry of the Keggin polyanions and effective van der Waals radii of 5.2 Å per sphere, the calculated packing density (the

DOI: 10.1021/ic502541b
Inorg. Chem. 2015, 54, 628−634

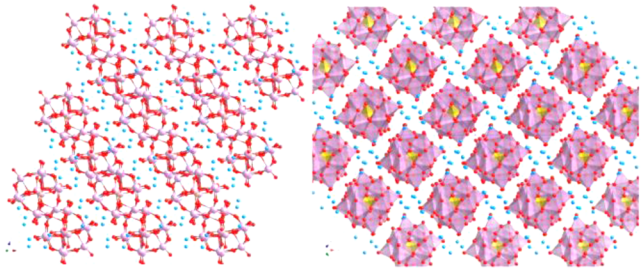

Figure 5. Crystal packing of **4** in a ball and stick model viewed along the *b* axis (left) and in a polyhedral model as projection of the {011} plane (right). Color code: M (Mo and V) pink, P yellow, and O red; structural water molecules are labeled blue for better representation.

fraction of the volume of the unit cell filled with spheres) would be 0.64, when the minimal possible packing density for regular lattice equals $\pi/(3\sqrt{2}) \approx 0.74$ as in case of *hcp* and *fcc* packing arrangements.[23] In contrast, structure **1** has a packing density of only 0.40. There are two polyanion spheres per unit cell, with eight water molecules per sphere. Compared with **3**, the spheres are shifted toward one another, forming a chess-like hexagonal arrangement. The volume of the unit cell has decreased even more, reaching 1833 Å^3 that is 916.5 Å^3 per sphere. Previously, this structure was proposed to exist as highly ordered intermediate phase[13] before the crystal of phosphovanadomolybdate becomes anhydrous, but it was never isolated.

The transformation of **1** to **4** and then further to an amorphous $H_5PV_2Mo_{10}O_{40}$ compound can also be followed in a continuous mode using powder X-ray diffraction, Figure 6.

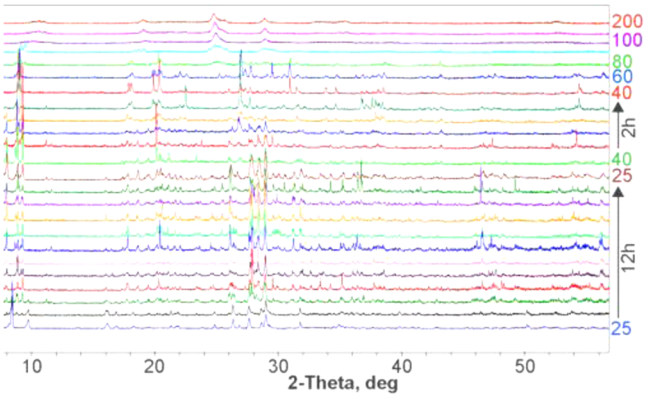

Figure 6. Powder XRD spectra of $H_5PV_2Mo_{10}O_{40}$ at various temperatures. The colors are used to differentiate between measurements. On the right axis, temperatures at which the diffraction pattern were measured are shown. The measured spectra of compounds **1** (blue 25 °C), **2** (brown 25 °C), and **3** (red 40 °C) fit the simulated diffraction patterns derived from single crystal diffraction data, Figures S4–S6, Supporting Information.

First the dehydration process of the transformation of **1** to **2** at 25 °C was followed over a period of 12 h after which the transformation appears to be complete. A limitation in following this transformation of **1** to **2** at 25 °C is that to get good diffraction patterns data acquisition needs to be lengthy. However, since the crystal transformations are occurring continuously, fast scan times were used that resulted in poor signal-to-noise ratios. Upon heating to 40 °C, **2** is transformed to **3** within less than 2 h where it is then stable. Upon further heating, the changes are quite rapid. The last crystalline diffraction pattern was obtained at 60 °C. The XRD pattern obtained at 60 °C is similar but is not exactly the pattern obtained for **3** or **4**. It is possible that even amore compact structure is formed, but we were unable to get reasonable single crystal data for analysis. Upon heating above 60 °C $H_5PV_2Mo_{10}O_{40}$ loses its crystallinity and is transformed to a mostly amorphous powder.

Rehydrated Structure. *$H_5PV_2Mo_{10}O_{40}\cdot 36H_2O$ (**5**).* An anhydrous polyoxometalate was prepared by heating the original sample at 100 °C for 24 h to yield a light orange powder, Figure 1C. This dried and amorphous solid was placed in a small closed vessel filled with water vapor as shown in Figure S3, Supporting Information. Almost immediately, the solid starts to adsorb water forming tiny droplets on its surface. From each of these droplets crystals were formed. After 2 h the entire material turned crystalline, and the X-ray structure of the compound **5** was measured. As can be seen from Table 1, this rehydrated compound is isostructural with the original wet crystal **1**, both molecularly, composition and the amount of water, and crystallographically, packing arrangement, space group, lattice constants, and so forth.

Organization of the Water. To further understand the differences among **1**–**4**, molecular graphics software, Hollow and PyMol,[19,20] was used to calculate and plot the surface of the interstitial space between Keggin polyanions, which is filled with water molecules, Figure 7. As can be seen from the figure,

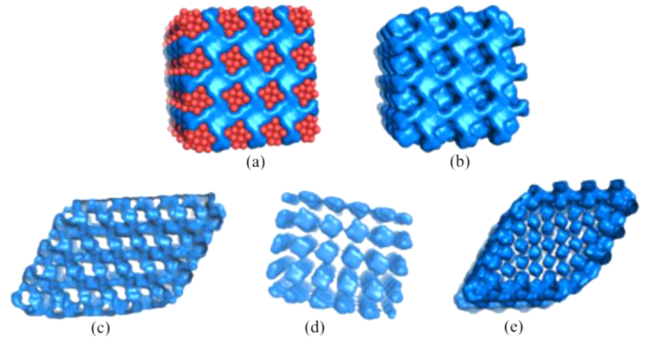

Figure 7. Surface of the interstitial spaces between the polyanions, which are filled with water molecules: (a) **1** with the polyanions; (b) **1** without the polyanions; (c) **2**; (d) **3**; (e) **4**.

the fully hydrated compound **1** can be visualized as spherical polyanion clusters "floating in the sea" of water molecules, Figure 7a,b. Already in the air-dried compound, **2**, Figure 7c, there is a dramatic change in the water content and its distribution. Water molecules are arranged in thin, ~2–3 Å, layers separating between the polyanions. These layers are aligned along the *a* axis. In the 40 °C dried compound **3**, Figure 7d, the water molecules are contracted into small rectangular pockets that are aligned along the *c* axis. Since all the water pockets are aligned the same direction, they appear to form an infinite channel-like structure. However, a closer examination reveals that these are not channels but rather singular rectangles that are separated by adjacent polyanions. The water molecules in **4**, Figure 7e, are also arranged in small pockets; however, compared with those in compound **3**, these pockets are smaller and shifted toward one another in such a way that they are not aligned but rather form a chess-like order between consecutive layers that allows a close-packed arrangement of the neighboring polyanions spheres.

In order to compare among all the structures and to emphasize the dramatic differences between the structures, the

DOI: 10.1021/ic502541b
Inorg. Chem. 2015, 54, 628–634

important parameters are summarized in Table 2. The crystals of $H_5PV_2Mo_{10}O_{40}$ undergo significant transformations during the dehydration process. About 40% squeeze in volume and the loss of more than 77% of structural water upon transformation from **1** to **4**, resulting in highly dense close packed structure. All these transformations proceed in solid state via a crystal-to-crystal process, and the most fascinating thing is that upon introduction of a humid atmosphere, the desiccated **4** regains back all its structural water molecules and returns to its fully hydrated form.

Table 2. Important Structural Parameters for 1−4

	1	2	3	4	5
cell volume (per polyanion), Å^3	1466.1	1045.1	939.9	916.6	1464.5
water molecules	36	14	8	8	36
packing density	0.402	0.564	0.627	0.643	0.402
distance between polyanions, Å	12.75	10.29	9.80	9.72	12.76

High Temperature Thermostructural Investigation. The thermal stability of $H_5PV_2Mo_{10}O_{40}$ was first investigated by thermogravimetric analysis (TGA). Characteristic TGA/DTA plots for **1** and **2**, Figure 8 and Figure S7, Supporting Information, show two main regions of weight loss that are correlated to two types of water molecules in these structures, (a) crystallization or solvated water that is released before ca. 150 °C and (b) constitutional water, that is, the protons bound to the polyanion surface oxygen atoms.[24] For both **1** and **2**, the experimentally observed weight losses of 27.35% and 12.46% at up to 150 °C correspond very well to the number of solvate water molecules, 36 (27.16 wt %) and 14 (12.67 wt %), respectively. The loss of solvated water is accompanied by multiple endothermic peaks in the corresponding regions of the DTA curves, Figure 8 and Figure S7, Supporting Information. For **1**, these peaks are more pronounced, the most noticeable transition being at ∼75 °C. These peaks are assigned to the stepwise dehydration processes that take place at these temperatures. Above these temperatures anhydrous $H_5PV_2Mo_{10}O_{40}$ was formed. At around 300 °C, an additional 2.5 water molecules are lost that can be assigned to the loss of constitutional water. In this process, acidic protons of $H_5PV_2Mo_{10}O_{40}$ are released together with lattice oxygen atoms. One may assume that also VO^{2+} cations are formed in a reductive elimination process. The vanadyl cations may compensate for the charge of the remaining polyanion core.[25] Above this temperature and up to 600 °C, no further weight loss was observed. There is an additional small exothermic peak at ∼435 °C that may correspond to crystallization of MoO_3 (see also below).[26]

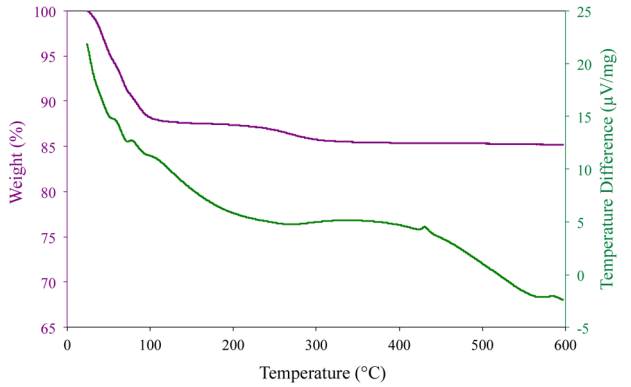

Figure 8. TGA (purple) and DTA (green) plots for **2**. Exothermic transformations are in the positive direction.

The thermal stability of $H_5PV_2Mo_{10}O_{40}$ was further studied by IR spectroscopy at temperatures ranging from 25 to 600 °C, Figure 9. The air-dried compound **2** has four strong characteristic peaks in the polyoxometalate region: 1060 cm^{-1} (P−O bond), 961 cm^{-1} (terminal M═O), and 864 and 778 cm^{-1} (edge and corner bridging M−O−M). As can be seen from Figure 9, the IR spectra remain essentially unchanged upon heating to 300 °C, indicating that $H_5PV_2Mo_{10}O_{40}$ is structurally stable within this temperature range. When heated beyond 300 °C, the molecular structure of $H_5PV_2Mo_{10}O_{40}$ begins to disintegrate. However, the process is relatively slow and even after 12 h at 400 °C, there is only partial decomposition of the Keggin polyanion. On the other hand, one can observe the appearance of new peaks at 991 cm^{-1} (s), 885 cm^{-1} (b), 817 cm^{-1} (w), and 598 cm^{-1} (b). At 500 °C already after 4 h the thermal transformation is completed and a new spectrum is obtained, which is then stable under prolonged heating up to 600 °C. For the sake of simplicity, $H_5PV_2Mo_{10}O_{40}$ calcinated or annealed at 500 °C is called **6**.

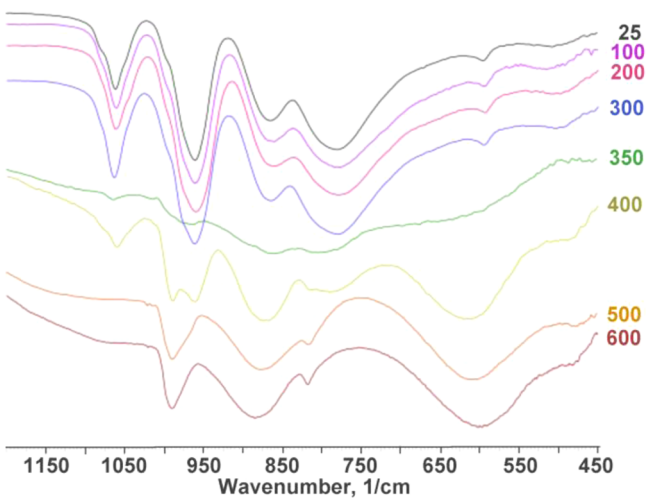

Figure 9. FT-IR transmission spectra of $H_5PV_2Mo_{10}O_{40}$ at various temperatures. The spectrum at 25 °C was taken as **2**, the spectrum at 400 °C was obtained after heating for 12 h, and the remaining spectra were obtained after heating for 4 h.

Calcinated $H_5PV_2Mo_{10}O_{40}$ was studied by various techniques. First one can see from the powder X-ray diffraction data, Figure 10, top, that a crystalline material was obtained that corresponds to orthorhombic MoO_3, molybdenum(VI) oxide (ICDD no. 05-0508). The measured lattice parameters were a = 3.954 Å, b = 13.929 Å, c = 3.685 Å, which is in good agreement with the literature values (a = 3.962 Å, b = 13.858 Å, c = 3.697 Å). Other crystalline materials that could have arisen from the degradation of $H_5PV_2Mo_{10}O_{40}$ such as V_2O_5, P_2O_5, or $VOPO_4$ were not detected by powder XRD. The Raman spectrum of **6**, Figure 10, middle, also coincides very well with that of MoO_3. Interestingly, however, the IR spectra of **6** and MoO_3 are somewhat different, Figure 10, bottom. In **6**, one can observe a small peak at 1020 cm^{-1}, which can be assigned to a P−O bond vibration. In addition, the contribution from the low frequency area is weaker for compound **6**.

DOI: 10.1021/ic502541b
Inorg. Chem. 2015, 54, 628−634

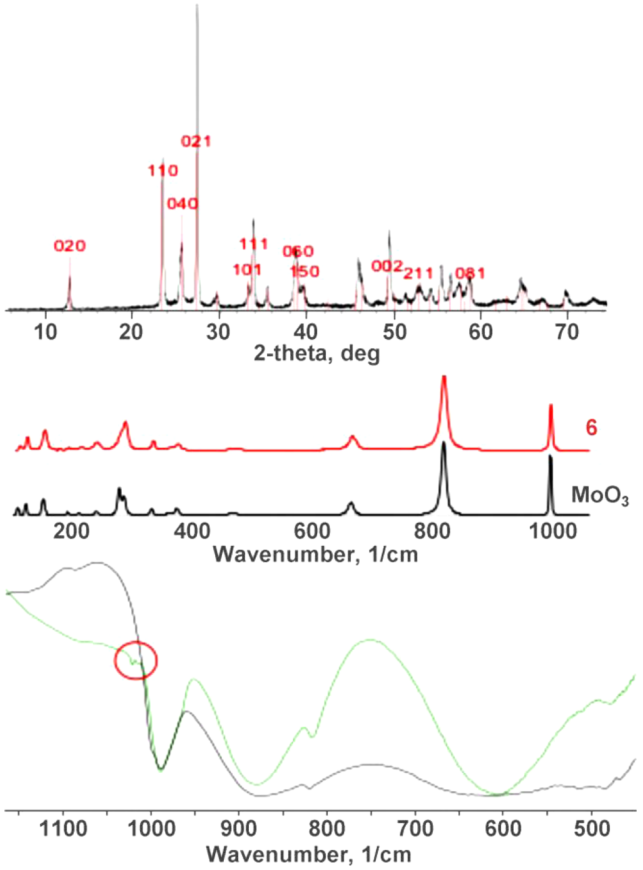

Figure 10. (top) Powder XRD diffraction pattern of **6** annealed for 16 h at 500 °C. The indexes in red correspond to those of MoO_3 from the ICDD database. (middle) Raman spectra of **6** (red) and MoO_3 (black). (bottom) FT-IR spectra of **6** (green) and MoO_3 (black).

Further characterization of $H_5PV_2Mo_{10}O_{40}$, **6**, was carried out using X-ray photoelectron spectroscopy, XPS. Careful examination of the *surface* composition of **6** (XPS is a surface sensitive technique, where the information is obtained from the top 10 nm of the surface) revealed the presence of vanadium, phosphorus, molybdenum, and oxygen atoms, Figure 11.

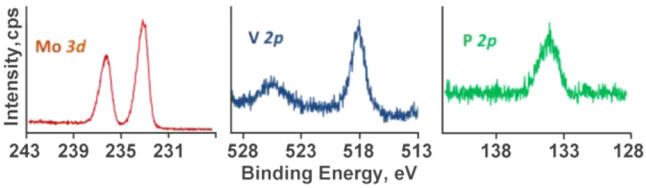

Figure 11. Original high resolution XPS spectra of **6** showing Mo 3d, V 2p, and P 2p regions.

Moreover, the average atomic ratios according to XPS results over four measurements was $P_{3.1}/V_{4.7}/Mo_{10}/O_{43.7}$, normalized to Mo. This indicates a large excess of vanadium and phosphorus atoms *on the surface* relative to molybdenum Mo atoms. Corresponding XPS analysis on the starting material, anhydrous $H_5PV_2Mo_{10}O_{40}$ showed a ratio of $P_{1.2}/V_{1.9}/Mo_{10}/O_{36.6}$, which is similar to the actual molecular composition. The binding energies of Mo $3d_{5/2}$ and Mo $3d_{3/2}$ appear at 233.1 and 236.2 eV, respectively, and are characteristic of Mo^{6+} in oxides. Similarly, V $2p_{3/2}$ and V $2p_{1/2}$ are located at 518.1 and 525.6 eV, respectively, and correspond to V^{5+} in oxides and P 2p appears at 134.1 eV, which is characteristic with P^{5+} in phosphates. The binding energies of anhydrous $H_5PV_2Mo_{10}O_{40}$ are essentially the same as the values noted above.

Beginning from anhydrous $H_5PV_2Mo_{10}O_{40}$, consecutive XPS measurements were also carried out on four additional samples of $H_5PV_2Mo_{10}O_{40}$ that were calcinated for 4 h at different temperatures. The plot of the atom ratio, V/Mo, as a function of the calcination temperature shows that the amount of vanadium on the surface gradually increased with increasing calcination temperature, that is, with the degree of degradation of the polyoxometalate, Figure 12.

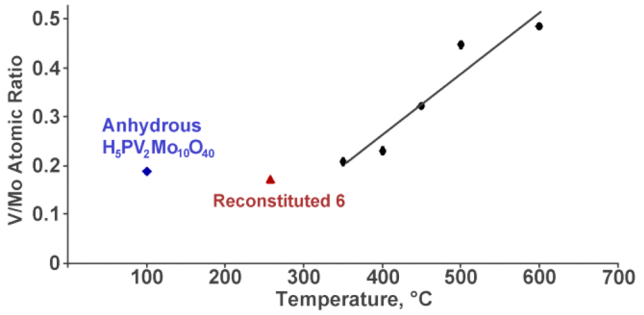

Figure 12. V/Mo atomic ratio obtained from XPS analysis of various samples of $H_5PV_2Mo_{10}O_{40}$: anhydrous, dried at 100 °C for 24 h (blue); calcinated at temperatures ranging from 350 to 600 °C for 4 h (black); after reconstitution of **6** (red).

The powder XRD, Raman, and IR results indicate that upon heating at 350 °C and above $H_5PV_2Mo_{10}O_{40}$ decomposed with formation of crystalline orthorhombic molybdenum oxide, MoO_3, with gradual enrichment of vanadium oxide and probably vanadyl phosphate on the surface as can be concluded from the XPS measurements. It is worth noting that the formation of P_2O_5 can be excluded because it sublimes at 360 °C and the binding energy for P 2p is higher, 135 eV.[27] The process of surface enrichment with vanadium is temperature dependent and corresponds to a reduction elimination process wherein VO^{2+} separates from the Keggin cluster, as was discussed previously.[25] The presence of vanadium oxide or vanadylphosphate was not detected by powder XRD. Likely they represent a dilute phase in the midst of a strongly diffracting phase and reasonably form amorphous or poorly crystalline phases.

Reconstitution of $H_5PV_2Mo_{10}O_{40}$. Since in heterogeneous catalysis applications of $H_5PV_2Mo_{10}O_{40}$ there could be degradation of the compound after heating for long periods of time, it is of interest to know whether the original polyoxometalate cluster could be reconstituted after its degradation. Thus, the brownish calcinated material **6** was dissolved in water and heated to 80 °C for 30 min, during which the solution turned orange. Quite surprisingly the ^{31}P and ^{51}V NMR spectra, Figure 13, clearly revealed that the original $H_5PV_2Mo_{10}O_{40}$ cluster was reconstituted in full. Evaporation of the solvent and measurement of the IR spectrum, Figure 13, as well as the XPS, Figure 11, also revealed that the original cluster was reformed. Interestingly perusal of the patent literature showed that an aqueous slurry of MoO_3, V_2O_5, and H_3PO_4 in appropriate amounts could form $H_5PV_2Mo_{10}O_{40}$ when refluxed for 20 days.[28] Here, the reaction with similar components occurs much more easily.

DOI: 10.1021/ic502541b
Inorg. Chem. 2015, 54, 628−634

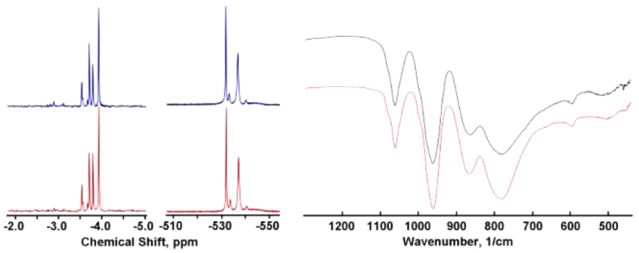

Figure 13. ^{31}P NMR (left), ^{51}V NMR (middle), and IR (right) spectra of original (top) and reconstituted (bottom) $H_5PV_2Mo_{10}O_{40}$. ^{31}P NMR peaks are at −3.58, −3.72, −3.76, −3.84, and −3.97 ppm; ^{51}V NMR peaks are at −532, −533, −537, and −540 ppm; IR peaks are at 16060, 911, 863, and 778 cm^{-1}.

CONCLUSIONS

At low temperature and in the solid state, $H_5PV_2Mo_{10}O_{40}$ shows the following rather unique crystal to crystal phase transitions. The initial crystallized 36-hydrate that has a cell volume of 1466.1 Å^3 per polyanion with a 12.75 Å distance between the polyanion clusters is stable only in its mother liquor and spontaneously loses water of hydration at 25 °C in air to yield a 14-hydrate with a nearly 30% more compacted structure. Heating only to 40 °C results in the further formation of an 8-hydrate with a cell volume of 939.9 Å^3 per polyanion and a 9.80 Å distance between the polyanion clusters. Interestingly, samples heated to 40−55 °C and whose crystal structure was measured at 120 K showed a further transformation to a nearly rhombohedral structure in which no additional water was lost but the reorganization of the water molecules in the secondary structure led to their chess-like organization. A high packing density of 0.64 was calculated comparable to closed packed structures with a density of 0.74. Importantly, in the presence of water vapor at room temperature, $H_5PV_2Mo_{10}O_{40}$ shows hygroscopic behavior and spontaneously rehydrates to form the original 36-hydrate. Powder XRD measurements show that crystallinity is lost above 60 °C with formation of an amorphous compound. Further thermogravimetric measurements showed that $H_5PV_2Mo_{10}O_{40}$ became anhydrous at ∼150 °C, but the $H_5PV_2Mo_{10}O_{40}$ cluster retains its structure indefinitely at up to 300 °C. Above this temperature, an additional 2.5 molecules of constitutional water is lost and a crystalline MoO_3 phase appears with formation of an amorphous vanadium oxide/vanadyl phosphate layer on the surface as observed by XPS. This transformation occurs at temperatures up to 600 °C. Importantly, the completely thermally decomposed $H_5PV_2Mo_{10}O_{40}$ cluster can be reconstituted quite simply by dissolution in water at 80 °C as shown by IR, ^{31}P NMR, and ^{51}V NMR. This is important also in the context of heterogeneous catalysis indicating that deactivated catalyst can rather simply be recovered by dissolution of a spent catalyst in water.

ASSOCIATED CONTENT

Supporting Information

Additional thermogravimetric, spectroscopic, and X-ray diffraction data. This material is available free of charge via the Internet at http://pubs.acs.org.

AUTHOR INFORMATION

Corresponding Author

*E-mail: Ronny.Neumann@weizmann.ac.il.

Notes

The authors declare no competing financial interest.

ACKNOWLEDGMENTS

This research was supported by the Israel Science Foundation Grant Nos. 1073/10 and 763/14, the Helen and Martin Kimmel Center for Molecular Design, and the Israeli Ministry of Industry and Trade. R.N. is the Rebecca and Israel Sieff Professor of Chemistry.

REFERENCES

(1) Pope, M. T. *Heteropoly and Isopoly Oxometalates*; Inorganic Chemistry Concepts; Springer-Verlag: Berlin, 1983; Vol. *8*.
(2) Okuhara, T.; Mizuno, N.; Misono, M. *Adv. Catal.* **1996**, *41*, 113−252.
(3) Kozhevnikov, I. V. In *Polyoxometalate Molecular Science*; Mueller, A., Pope, M. T., Eds.; Kluwer Academic Publishers: Dordrecht, the Netherlands, 2003; pp 351−380.
(4) Misono, M. *Catal. Rev. Sci. Eng.* **1987**, *29*, 269−321.
(5) Jerschkewitz, H. G.; Alsdorf, E.; Fichtner, H.; Hanke, W.; Jancke, K.; Öhlmann, G. Z. *Anorg. Allg. Chem.* **1985**, *526*, 73−85.
(6) Sasca, V.; Stefanescu, M.; Popa, A. *J. Therm. Anal. Calorim.* **1999**, *56*, 569−578.
(7) Mestl, G.; Ilkenhans, T.; Spielbauer, D.; Dieterle, M.; Timpe, O.; Krohnert, J.; Jentoft, F.; Knozinger, H.; Schlogl, R. *Appl. Catal., A* **2001**, *210*, 13−34.
(8) (a) Bielanski, A.; Malecka, A.; Kybelkova, L. *J. Chem. Soc., Faraday Trans. 1* **1989**, *85*, 2847−2856. (b) Rocchiccioli-Deltcheff, C.; Fournier, M. *J. Chem. Soc., Faraday Trans.* **1991**, *87*, 3913−3920.
(9) Günter, J. R.; Bensch, W. *J. Solid State Chem.* **1987**, *69*, 202−214.
(10) (a) Iturrospe, A.; San Felices, L.; Reinoso, S.; Artetxe, B.; Lezama, L.; Gutiérrez-Zorrilla, J. M. *Cryst. Growth Des.* **2014**, *14*, 2318−2328. (b) Iturrospe, A.; Artetxe, B.; Reinoso, S.; San Felices, L.; Vitoria, P.; Lezama, L.; Gutiérrez-Zorrilla, J. M. *Inorg. Chem.* **2013**, *52*, 3084−3093.
(11) Kozhevnikov, I. V. *Catalysis by Polyoxometalates*; Wiley: Chichester, U.K., 2002.
(12) (a) Neumann, R.; Khenkin, A. M. *Chem. Commun.* **2006**, 2529−2538. (b) Neumann, R. *Inorg. Chem.* **2010**, *49*, 3594−3601.
(13) Herzog, B.; Bensch, W.; Ilkenhans, Th.; Schlögl, R.; Deutsch, N. *Catal. Lett.* **1993**, *20*, 203−219.
(14) Fournier, M.; Feumi-Jantou, C.; Rabia, C.; Hervé, G.; Launay, S. *J. Mater. Chem.* **1992**, *2*, 971−978.
(15) Tsigdinos, G. A.; Hallada, C. J. *Inorg. Chem.* **1968**, *7*, 437−441.
(16) Otwinoski, Z.; Minor, W. *Methods Enzymol.* **1997**, *276*, 307−326.
(17) Sheldrick, G. M. *Acta Crystallogr.* **2008**, *A64*, 112−122.
(18) Emsley, P.; Lohkamp, B.; Scott, W. G.; Cowtan, K. *Acta Crystallogr.* **2010**, *D66*, 486−501.
(19) Bosco, K. H.; Gruswitz, F. *BMC Struct. Biol.* **2008**, *8*, No. 49.
(20) The PyMOL Molecular Graphics System, Version 1.7.1, Schrödinger, LLC, 2014.
(21) Evans, H. T.; Pope, M. T. *Inorg. Chem.* **1984**, *23*, 501−504.
(22) Sergienko, V. S.; Korai-Koshits, M. A.; Yurchenko, E. N. *Zh. Struk. Khim.* **1980**, *21*, 111−125.
(23) Conway, J. H.; Sloane, N. J. A. *Sphere Packings, Lattices, and Groups*, 2nd ed.; Springer-Verlag: New York, 1993.
(24) West, S. F.; Audrieth, L. F. *J. Phys. Chem.* **1955**, *59*, 1069−1072.
(25) (a) Taouk, B.; Ghoussoub, D.; Bennani, A.; Crusson, E.; Rigole, M.; Aboukais, A.; Decressain, R.; Fournier, M.; Guelton, M. *J. Chim. Phys. Phys.-Chim. Biol.* **1992**, *89*, 435−444. (b) Brueckner, A.; Scholz, G.; Heidemann, D.; Schneider, M.; Herein, D.; Bentrup, U.; Kant, M. *J. Catal.* **2007**, *245*, 369−380.
(26) (a) Rode, E. Y.; Sokolova, M. P. *Russ. J. Inorg. Chem.* **1963**, *8*, 980−983. (b) Marchal, C.; Davidson, A.; Thouvenot, R.; Hervé, G. *J. Chem. Soc., Faraday Trans.* **1993**, *89*, 3301−3306.
(27) Wang, Y.; Sherwood, P. M. A. *Surf. Sci.* **2002**, *9*, 159−165.
(28) Takeru, O.; Masayuki, O. US Patent 4146574, 1979.

DOI: 10.1021/ic502541b
Inorg. Chem. 2015, 54, 628−634